Genetic diversity loss in a biodiversity hotspot: ancient DNA quantifies genetic decline and former connectivity in a critically endangered marsupial

Carlo Pacioni[1], Helen Hunt[1], Morten E. Allentoft[1,2], Timothy G. Vaughan[3], Adrian F. Wayne[4], Alexander Baynes[5], Dalal Haouchar[1], Joe Dortch[6] and Michael Bunce[1,7*]

[1]Ancient DNA laboratory, School of Veterinary and Life Sciences, Murdoch University, Murdoch, WA 6150, Australia.

[2]Centre for GeoGenetics, Natural History Museum, University of Copenhagen, Øster Voldgade 5-7, 1350 Copenhagen K, Denmark.

[3]Department of Computer Science, University of Auckland, Auckland, New Zealand

[4]Department of Parks and Wildlife, Manjimup, WA 6258, Australia.

[5]Western Australian Museum, Locked Bag 49, Welshpool DC, WA 6986, Australia.

[6]Archaeology, M257, The University of Western Australia, 35 Stirling Highway, Nedlands, WA 6009, Australia.

[7]Trace and Environmental DNA laboratory, Department of Environment and Agriculture, Curtin University, Perth, WA 6845, Australia.

* Corresponding author: michael.bunce@curtin.edu.au

Abstract

The extent of genetic diversity loss and former connectivity between fragmented populations are often unknown factors when studying endangered species. While genetic techniques are commonly applied in extant populations to assess temporal and spatial demographic changes, it is no substitute for directly measuring past diversity using ancient DNA (aDNA). We analysed both mitochondrial DNA (mtDNA) and nuclear microsatellite loci from 64 historical fossil and skin samples of the critically endangered Western Australian woylie (*Bettongia penicillata ogilbyi*), and compared them with 231 (*n*=152 for mtDNA) modern samples. In modern woylie populations 15 mitochondrial control region (CR) haplotypes were identified. Interestingly, mtDNA CR data from only 29 historical samples demonstrated 15 previously unknown haplotypes and detected an extinct divergent clade. Through modelling, we estimated the loss of CR mtDNA diversity to be between 46% and 91% and estimated this to have occurred in the past 2000-4000 years in association with a dramatic population decline. Additionally, we obtained near-complete 11-loci microsatellite profiles from 21 historical samples. In agreement with the mtDNA data, a number of 'new' microsatellite alleles was only detected in the historical populations despite extensive modern sampling, indicating a nuclear genetic diversity loss greater than 20%. Calculations of genetic diversity (heterozygosity and allelic rarefaction) showed that these were significantly higher in the past and that there was a high degree of gene flow across the woylie's historical range. These findings have an immediate impact on how the extant populations are managed and we recommend the implementation of an assisted migration program to prevent further loss of genetic diversity. Our study demonstrates the value of integrating aDNA data into current-day conservation strategies.

Keywords: ancient DNA, population bottleneck, biodiversity loss, genetic diversity, Bettongia

Introduction

Species and populations that are adversely affected by anthropogenic activities, including habitat modification, are a global phenomenon (Andrén 1994; Ewers & Didham 2006). The reduction in genetic diversity, often associated with population bottlenecks and habitat fragmentation, can result in the loss of reproductive fitness and reduction in evolutionary potential (Frankham 1996; Frankham *et al.* 1999). Genetic bottlenecks are most commonly studied using modern molecular data and theoretical models are applied to determine their likelihood and severity (Cornuet & Luikart 1996; Garza & Williamson 2001). The incorporation of time-stamped ancient DNA (aDNA) data, for example obtained from museum skins and fossils, can provide direct insight into a population's past diversity (Ramakrishnan & Hadly 2009). The demographic history of bison (Shapiro *et al.* 2004), musk ox (Campos *et al.* 2010) and the collared lemming (Brace *et al.* 2012), for example, have been extensively studied using mitochondrial DNA (mtDNA) isolated from preserved fossil material. However, the use of aDNA data to make informed conservation decisions is rare, despite the fact that it can provide vital information regarding past population demography (e.g. bottlenecks), former connectivity and extent of genetic diversity (see Leonard 2008 for a review).

An Australian example of a species adversely affected by population declines is the woylie (or brush-tailed bettong, *Bettongia penicillata ogilbyi*). Woylies are critically endangered, nocturnal marsupials (Groom 2010; Wayne *et al.* 2008a), that feed primarily on hypogeal

fungi (native truffles), tubers, bulbs, seeds and invertebrates, and they weigh between 1.1 and 1.6 kg (Van Dyck & Strahan 2008). With the exception of five translocated sites (i.e. not naturally occurring) in South Australia and New South Wales, the distribution of the woylie is currently limited to the south-west region of Western Australia (WA), one of only 34 recognised biodiversity hotspots on the planet (Myers *et al.* 2000). Historically, together with the subspecies *B. p. penicillata*, this species had a widespread distribution across southern Australia, but since European settlement (in the 18th century), it has undergone a substantial population decline (Fig. 1), attributed primarily to the introduction of feral predators, particularly red foxes (*Vulpes vulpes*) (Burbidge & McKenzie 1989; Start *et al.* 1998; Woinarski *et al.* 2015). Habitat fragmentation and changes in fire regimes have also been suggested as contributing factors (Groom 2010). An example of the extent of land clearing in the woylie's former range is the "Wheat-belt" region, an area of 95,800 km^2 about the size of Portugal , whereonly ~7% of the original vegetation remains in a number of small isolated pockets (Saunders 1979).

Despite a spectacular recovery in the 1990s due to the intensification of the control of the red fox (Start *et al.* 1998), the woylie has undergone a second, more recent, decline, resulting in a 90% reduction in seven years from a peak of about 200,000 animals in 1999 (Wayne *et al.* 2013). The factors responsible for this decline are still not well defined (Groom 2010; Wayne *et al.* 2015). Recent genetic studies of the extant populations using microsatellite data from 231 live individuals revealed four genetically distinct wild populations (Pacioni *et al.* 2011). Two of these are found in the highly fragmented Wheat-belt region: Dryandra woodland and Tutanning Nature Reserve and the other two within the Upper Warren region; Kingston and Perup (Fig. 1). Current size estimates in these naturally occurring populations (excluding

93 translocated populations) are approximately <10,000, with Tutanning Nature Reserve having
94 gone extinct in the wild in 2011 (Wayne *et al.* 2013, Department of Parks and Wildlife
95 unpublished data). Woylie translocated populations account for another ~4,000 individuals
96 (Wayne *et al.* 2013).
97
98 An evaluation of contemporary genetic diversity among 152 modern individuals from the four
99 remnant populations, using the mitochondrial control region (CR), revealed 15 haplotypes,
100 and expected heterozygosity (H_E, n=231) values of 63-83% for 12 microsatellite loci (Pacioni
101 *et al.* 2011). However, it is unknown to what extent genetic diversity has been lost since the
102 collapse of the population. The use of heterozygosity values calculated only from modern
103 samples as a measure of genetic health can be problematic due to the lack of comparative
104 baseline data. A direct assessment of genetic diversity using both pre- and post-decline
105 samples is the only way to securely quantify genetic diversity changes over time with any
106 degree of accuracy. An appreciation for temporal effects is often a missing factor when
107 making conservation decisions, the woylies being a case in point where, for example, the lack
108 of baseline data makes the establishment of conservation targets difficult (Pacioni *et al.*
109 2013). In this study, we used the woylie as an example to investigate to what extent the
110 application of aDNA techniques can improve our understanding of the dynamics associated
111 with wildlife declines. We characterised two genetic markers: mitochondrial DNA (control
112 region and cytochrome *b*) and microsatellites, and assessed the possible loss of the genetic
113 diversity and the degree of historical gene flow between regions. We further discuss how the
114 information obtained can inform conservation decisions.
115

116 # Materials and methods

Skin and Bone Sampling

A total of 64 historical samples were sourced from the collections of the Western Australian Museum (WAM). Samples included fossil bone fragments from vertebrate archaeological collections (*n*=15), museum skins (*n*=28) and bone material from the vertebrate palaeontological collection (*n*=21) ranging between ~40 and 15,600 years old (Dortch 2004a; b, Table S1 supporting information). Samples represent a wide geographical area, with coverage across woylie former distribution (Fig. 1). The entire WAM woylie skin collection was sampled for this study. Woylie fossils, from across southern WA, were selected from sites such as caves that are typically conducive to long-term DNA preservation.

DNA Extraction

DNA extractions from historical samples were carried out in a dedicated aDNA laboratory located at Murdoch University (Perth, Australia), minimising contamination from PCR amplicons and modern DNA in accordance with established aDNA guidelines (Gilbert *et al.* 2005). Skin samples with attached hair (~5x5 mm) were diced using a sterile scalpel blade and incubated overnight at 55°C with rotation, in 500 µl of digest buffer (20 mM Tris; pH 8, 1% SDS, 5 mM $CaCl_2$, 10 mM dTT, and 10 mM EDTA) with the addition of 10 mg of Proteinase K (Invitrogen). DNA was bound and eluted from the digest buffer using DNeasy blood and tissue kit according to the manufacturer's recommendations (Qiagen). Samples of bone and teeth were grounded to powder using a Dremel tool (part no. 114; Germany) set at a low speed. Approximately 100 mg of bone powder was incubated in a bone digest buffer (containing; 20 mM Tris; pH 8, 1% SDS, 10 mM dTT, 0.48 M EDTA and 10 mg of Proteinase K) overnight at 55°C with rotation. Following digestion, all tissue samples were centrifuged briefly to pellet debris and the supernatant transferred to a Vivaspin 500 tube with a 30,000 Dalton molecular weight cut-off membrane (Sartorius Stedim Biotech) and

centrifuged at 13,000 rpm, until ~50 µl of supernatant remained. This was then mixed with five volumes of PBI buffer (Qiagen) and DNA was extracted using a DNeasy tissue and blood kit (Qiagen) according to the manufacturer's recommendations.

DNA quantification

Following extraction, each sample was assayed for DNA preservation using quantitative PCR (qPCR) assays. The ability to successfully genotype nuclear aDNA loci is largely dependent on template copy number (Allentoft *et al.* 2011), accordingly qPCR assays represent an important step in determining relative preservation across a set of samples such as collected here.

The mtDNA primers targeting the 12s rRNA region (12s woylie macro 302F, primer sequence CGTAAAGCGTGTTTAAGCC and 12s woylie macro 425R, primer sequence CTGTAGTGTATTCAGCAAA; PCR product ~120 bp) were tested and shown to function well in a SYBR-bead qPCR assay and therefore used to screen all samples. The PCR reagents and protocol were optimised with a final 25 µl PCR reaction consisting of 2 µl template DNA, 3.0 mM $MgCl_2$ (Fisher Biotech, FB), 1x PCR buffer (FB), 0.5 mM each dNTP's (Astral Scientific), 0.16 µmoles of each primer (12s 302F/425R), 0.6 µl of SYBR Green dye (Stock 1/10,000 dilution; Invitrogen), 0.25 U AmpliTaq Gold polymerase (Life Technologies) and 1 µl (10 mg/mL) bovine serum albumin (BSA) (Fisher Biotech). PCR conditions were an initial hot start at 95°C for 5 min followed by 40 cycles of 95°C for 45 sec, 57°C for 45 sec and 72°C for 45 sec. The same qPCR assay was used to assess the relative quantity of DNA in all the historical DNA extracts, to establish the relative copy number of each sample. While many of the "failed" samples still yielded DNA (Table S1), they were excluded from the

analyses because of problems associated with allelic dropout of microsatellite loci — a phenomenon commonly encountered with degraded DNA (Allentoft *et al.* 2011; Bouzat *et al.* 1998; Taylor *et al.* 1994).

DNA amplification

A ~400 bp fragment of the CR and a 370 bp fragment of the cytochrome *b* gene were amplified using primers designed to target specific mtDNA regions (Table S2, Supporting information). Reactions typically consisted of a 25 µl reaction containing 2 µl template DNA, 2 mM $MgSO_4$, 1x PCR buffer, 0.25 mM each dNTP's, 8 ρmoles of each primer, 0.25 U HiFi Taq polymerase (Invitrogen), 1 µl (10 mg/mL) bovine serum albumin and template DNA. PCR conditions were: a hot start at 95°C for 5 min followed by 40 cycles of 95°C for 45 sec, 56°C/58°C (depending on primer set used) for 45 sec and 68°C for 45 sec. DNA was sequenced in both directions using dye terminator cycle sequencing chemistry (3730xl sequencer; Applied Biosystems via Macrogen - BigDye ver 3.1). Sequences were aligned in Geneious Pro (BioMatters). PCR repetitions using varying amounts of input DNA were conducted on individuals with unique mutations in order to check sequence fidelity. In addition, those fragments with unique mutations were cloned using the p-GEM "TA" vector system (Promega) to verify these rare variants and to investigate whether they could be accounted for by post-mortem DNA damage (primarily the deamination of cytosine, causing a C to T change during PCR amplification) (Briggs *et al.* 2007; Willerslev & Cooper 2005).

The microsatellite loci targeted in this study were previously used to characterise modern woylie genetic diversity (Table S3; Pacioni & Spencer 2010), with the exclusion of Y151 due to large variation in amplicon product size at this locus. All microsatellite amplifications were

conducted as described above except that Amplitaq Gold polymerase (Applied Biosystems) was used and 1.25 mM $MgCl_2$. Primers for two loci (Y175 and Bt76) were redesigned closer to the microsatellite repeating unit in order to shorten the allele length and reduce allelic dropout.

DNA fragment analysis of the amplified microsatellite products was carried out using a 5-dye system on an Applied Biosystems 3730 DNA analyser. The PCR product size was determined using an internal size standard (Genescan TM-500 Liz; Applied Biosystems) and fragments were scored using GeneMarker software (v1.5, Soft Genetics). Genotyping was repeated at least three times for homozygotes, with the addition of different starting amounts of DNA and were accepted only when all three repeats were homozygous for the same allele and, similarly, heterozygotes were repeated twice and accepted when both were heterozygous for the same alleles. We calculated the frequencies of falsely scoring an individual as homozygous ($P_{(fh)}$, Gagneux *et al.* 1997) and then the probability of falsely scoring an individual (per locus) given our protocols (i.e. $P_{(fh)}^3$). Two modern samples were co-run in each PCR to ensure direct comparability between the modern and historical datasets, and the allele scores of microsatellites from redesigned primer pairs were adjusted accordingly.

Mitochondrial DNA data analysis

Haplotypes from the historical samples were identified with DNAsp (Librado & Rozas 2009), which was also used to calculate haplotype (h) and nucleotide diversity (π) (Nei 1987). We applied the Stirling probability distribution to calculate the posterior probability of the expected total number of (historical) haplotypes (Dixon 2006). As a result, we calculated the probability that additional haplotypes were yet to be sampled, and estimated the expected total

number of historical haplotypes, based on the observations and sample size of the historical data. Sequences from modern data with complete coverage of the region amplified from historical samples (n=146) were obtained from Pacioni *et al.* (2011), and their h and π values were compared with those obtained from historical samples using a t-test. Rarefaction curves from both historical and modern datasets were calculated using Vegan (Oksanen *et al.* 2013) in R v2.15 (R DevelopmentCore Team 2015) and plotted to allow graphical comparison of haplotype richness between the two datasets. The haplotype richness obtained with the rarefaction approach allows for a direct comparison between the "modern" and "ancient" datasets because it standardises the sampling effort. To further explore the expected number of historical haplotypes, we fitted the two- and three-parameter asymptotic exponential models to the haplotype richness data, compared them with the F-test, and then predicted, using the most supported model, the number of historical haplotypes that we would have obtained had we had available the same number of samples as for the modern data. Spatial-temporal changes in the mtDNA genetic diversity were also visualised with a multi-dimensional parsimony network built in TempNet v1.8 (Prost & Anderson 2011).

The CR and cytochrome *b* sequence alignments were analysed with the Bayesian methods implemented in BEAST v1.5.3 (Drummond & Rambaut 2007) to obtain the phylogenetic relationships. The general time-reversible (GTR) model of nucleotide substitution with invariant and gamma sites (I+G), was used as determined by Modeltest v3.7 (Posada & Crandall 1998). A strict molecular clock was assumed. The northern bettong (*Bettongia tropica*, GENBANK accession numbers AF287895–AF287906) is a sister taxon to *B. penicillata* and was therefore used to root the tree. To place the woylie radiation in a temporal context, the cytochrome *b* sequences, along with other marsupial sequences (Genbank

237 accession numbers in Table S4), were modeled in BEAST using the GTR+I+G substitution
238 model, assuming a strict molecular clock and Yule process speciation, and enforcing two
239 published calibrations (Westerman *et al.* 2004). A calibration of 23.8 million years (95% CI
240 23.0-25.9), for the divergence between the Macropodinae and the Potoroinae, and of 8.3
241 million years (95% CI 5-12) for divergence of *Bettongia* were imposed. Three runs of ten
242 million generations (sampling every 1000 trees) were conducted and combined using
243 LogCombiner v1.5.3. After a burn in of 1000 trees per run, a consensus tree was generated
244 using TreeAnnotator v1.5.3.
245
246 Next, we evaluated changes of woylie population size over time using coalescent-based
247 approaches as these have proven efficient in detecting demographic changes (Peery *et al.*
248 2012). We analysed the woylie CR mtDNA data using BEAST v.1.8 (Drummond *et al.* 2012)
249 running 200 million iterations and discarding the first 10% as burn in. We used the estimated
250 dates of the aDNA samples and calibrated the root with a lognormal prior using the results of
251 the analysis of the cytochrome *b* dataset described above. We used a lognormal prior also for
252 the clock rate while leaving default options for the remaining priors. Using the Akaike
253 information criterion through Markov chain Monte Carlo (AICM, Baele *et al.* 2012) with 1000
254 bootstraps, we compared three demographic models: constant population size, exponential
255 growth and Bayesian Skyline Plot (BSP). Appropriate mixing and estimated sample size in the
256 analyses was checked with Tracer v.1.6 (Rambaut & Drummond 2007).
257
258 We also used a structured coalescent sampler to analyse these data to account for potential
259 problems arising from population structuring (Ho & Shapiro 2011; Navascués *et al.* 2010). The
260 historical data for these analyses were limited to samples that were geographically close to the

extant populations (n=13). Using Migrate-n v3.6.8 (Beerli 2006), we compared migration models of different levels of complexity: we started from a full model where the four populations (Tutanning, Dryandra, Kingston and Perup) were kept separate. Because of their relative geographic position, direct migration from Tutanning to any of the Upper Warren populations (and vice versa) was prevented (i.e. animals from Tutanning could only migrate to Dryandra and vice versa). We considered two three-population models where in one the two populations from the Wheat-belt region (Dryandra and Tutanning) were merged into one population and Perup and Kingston kept separate and, in the second, the Perup and Kingston were merged and the Wheat-belt populations were kept separate. We further simplified the migration model by considering only two populations (one for each region) and lastly we simulated a panmictic population. These analyses were conducted running 10 replicates of 400 million iterations, sampling every 2000 trees and discarding 30% of the trees as burn-in. Each analysis ran four chains with the default static heating scheme using slice sampling (Neal 2003) and with a gamma prior for both population parameters (Θ: 0.2, 0.06, M: 500, 0.5). Eventually, models were compared using the log Bayes Factor (LBF) calculated with the Bezier marginal likelihoods obtained by thermodynamic integration. Once the migration model was selected, we used Migrate-n to generate BSPs. Appropriate mixing and estimated sample size in Migrate-n analyses as well as post-analysis data plotting was carried out with the R package mtraceR (https://github.com/carlopacioni/mtraceR). To evaluate the extent of the bias introduced in BEAST where substructuring was not explicitly taken into account, we generated a BSP using BEAST with the same input file used for Migrate-n (i.e. limiting the historical samples to geographically close to the extent populations, n=13) and graphically compared the results. Where relevant, we repeated the demographic analysis with modern data only to evaluate whether the addition of aDNA data had substantially changed our results.

285

286 *Microsatellite data analysis*

287 The microsatellite data do not strictly conform to the requirements for testing the Hardy-
288 Weinberg Equilibrium, as they do not represent a population in the same space and time
289 (Frankham *et al.* 2002). Too few samples were available from one location during the same
290 time to test meaningfully whether genotype frequencies were in Hardy-Weinberg proportions.
291 Therefore, the data prevented identifying and correcting genotyping errors based on
292 deviations from Hardy-Weinberg proportions, as well as deficiencies and excesses of
293 particular genotypes using these standard approaches (e.g. Kalinowski 2006). However,
294 allelic dropout was identified from PCR replications of historical samples.

295

296 Descriptive measures of genetic diversity were calculated in GENALEX v6.2 (Peakall &
297 Smouse 2006), which included measures of allelic frequency per locus, observed
298 heterozygosity (H_o) and observed number of alleles (N_A).

299

300 Historical data were compared with modern data obtained from Pacioni *et al.* (2011) to
301 identify alleles that were not present in the modern data (unique alleles). Because differences
302 in sampling intensity can bias comparison of genetic diversity, with datasets containing larger
303 number of samples expected to contain more alleles (Kalinowski 2004), we used rarefaction
304 to compensate for the differences in sampling effort and calculated the number of alleles
305 present in an increasing sample size (from 1 to 20 for the historical dataset and from 1 to 210
306 samples for the modern data) using PopGenKit (Rioux Paquette 2011) in R v2.15 (R
307 DevelopmentCore Team 2015) and plotted the rarefaction curves for each dataset. Similarly
308 to what we did with the mtDNA data, we fitted the two- and three-parameter asymptotic

309 exponential models to the haplotype richness data, compared them with the *F*-test, and then
310 predicted, using the most supported model, the number of historical haplotypes that we would
311 have obtained had we had available the same number of samples as for the modern data.
312 Moreover, we compared allelic richness, obtained sampling 11 diploid individuals, between
313 the modern and historic data with the non-parametric Wilcoxon signed-rank test (Kalinowski
314 2004). We also compared the individual *IH* between the two datasets with Mann-Whitney
315 test. Furthermore, to investigate possible differences in connectivity between regions we
316 estimated the number of migrants using the "private allele" (the alleles found exclusively in
317 one population) method (Barton & Slatkin 1986) and used GENEPOP v4.2 (Rousset 2008)
318 for this purpose. We selected this method because its assumptions are not violated by
319 heterochronous data. However, we acknowledge that the number of migrants estimated with
320 this approach is possibly biased due to the fact that most private alleles would also be rare
321 and, therefore, may be lost during population declines (i.e. the number of migrants calculated
322 from the modern dataset would be inflated). For the latter analysis, data from the two woylie
323 populations in the Upper Warren region were merged because records did not specify whether
324 historical samples were collected from the eastern or western compartment of the Upper
325 Warren forest. One locus was omitted from all statistical comparisons: Y112, due to high
326 rates of allelic dropout evident from PCR repetitions (see below). All univariate statistical
327 analyses were performed with SPSS v19 (IBM. 2010) or R v2.15 (R DevelopmentCore Team
328 2015).
329
330 Evidence of population bottlenecks for each extant population was investigated, using modern
331 microsatellite data, by testing for excess in heterozygosity (Cornuet & Luikart 1996) and
332 mode-shift (Luikart & Cornuet 1998), with the program BOTTLENECK (Piry *et al.* 1999). A

mixed model of microsatellite mutation was assumed, with single step mutations accounting for 95% of all mutation events and a variance among multiple steps of 12 (Piry *et al.* 1999). We used a Wilcoxon signed-rank test to test statistical significance (Piry *et al.* 1999). We also used the M-ratio method with M_P_VAL, using recommended mutation parameters: 0.2 for the proportion of one-step mutations (p_s), 3.5 as the average size of non one-step mutations (Δ_g) and a mutation rate (μ) of $5x10^{-4}$/locus/generation (Garza & Williamson 2001). It was assumed that the population census sizes (N_c) prior to European settlement were similar to those estimated at the peak density observed after the commencement of the fox control program, immediately prior to the most recent declines (i.e. a conservative and best available estimate of pre-European populations) (Groom 2010). Following Frankham (1995), we approximated effective population size (N_e) to be 10% of N_c. Tutanning pre-European settlement N_e was assumed to be similar to the N_e at Dryandra. This test is anticipated to produce positive results for at least 100 generations post-reduction (Garza & Williamson 2001).

Lastly, we used Migrate-n to estimate demographic changes over time after having determined an appropriate migration model with the same approach as outlined for the mtDNA data. Microsatellite data were analysed with an exponential prior (Θ: 300; M: 1000) and running 4 replicates of 100 million iterations, sampling every 1250 trees and discarding 25% of the trees as burn-in. Each analysis ran four chains with the default static heating scheme using slice sampling (Neal 2003).

Results

356 *DNA recovery and quantification*

357 Of the 64 samples tested, including historical skins and fossils bones, DNA was successfully
358 isolated from 49 samples (76.5% success, Table S1). However, we specifically focused on a
359 subset of 29 well preserved samples, as determined by relative qPCR cycle threshold (C_T)
360 values (C_T is the number of cycles that are needed to obtained a pre-determined fluorescent
361 intensity and are inversely proportional to the initial amount of template used in the
362 reactions), spanning the entire former range of the woylie. There were two reasons to focus on
363 this subset of samples: firstly, we wanted to minimise the effect of microsatellite allelic drop
364 out often encountered with low copy number DNA (Allentoft *et al.* 2011); secondly, samples
365 with good DNA preservation are less prone to artefacts such as contamination and DNA
366 damage.

367

368 Skin samples had relatively better DNA preservation than fossil bone, with a mean ΔC_T value
369 of 4.24 or 18.9 times more DNA (25.55±5.90 SE compared to 29.77±5.79). Likewise,
370 younger samples yielded more mtDNA quantities than older samples (Table S1. See also
371 Hunt 2010). Although there was substantial variation in preservation, as expected (Allentoft
372 *et al.* 2012), there was a general trend with older specimens having lower relative DNA
373 concentrations, presumably due to a longer exposure to hydrolytic and enzymatic processes
374 (Allentoft *et al.* 2012). Lastly, as previously observed (Allentoft *et al.* 2011), there was an
375 overall trend between the C_T values and the percentage of microsatellite loci that could be
376 typed (Fig. S1).

377

Mitochondrial DNA analysis

The lengths of the CR sequences obtained from the 29 historical samples varied between 250 and 400 bp (excluding primers). While all of these were used for phylogenetic analysis (see below), we limited statistical analysis to 23 historical samples of ~400 bp (Table S1). Among these 23 historical samples (of which ~70% were around 100 years old or less, see Table S1), we identified a total of 18 haplotypes. Six samples possessed four CR haplotypes that are still present in extant populations. The remaining 15 haplotypes have not previously been observed despite intensive sampling of the modern woylie populations (Pacioni *et al.* 2011). These differences are further highlighted in the multidimensional network (Fig. 2).

Haplotype and nucleotide diversity of the sequences obtained from historical data was 0.976 (SD=0.02) and 0.039 (SD=0.004), which was substantially higher than any of the values calculated from the extant wild populations (range: h=0.26-0.82; π=0-0.022. Pacioni *et al.* 2013), and significantly higher than that obtained from the modern dataset (h=0.735, SD=0.001, p<0.001; π=0.022, SD=0.002, p<0.001).

The rarefaction curve computed from the historical dataset had a much higher trajectory and did not plateau, suggesting that there were many unsampled historical haplotypes (Fig. 3a). The three-parameter asymptotic exponential model was a significantly better fit (p<0.002) than the two-parameter model and predicted an expected number of haplotypes equal to 42.4 if 146 historical samples had been used (equation: $nh = 43.97 - 0.02\ e^{3.78\ S}$, where nh is expected number of haplotypes, and S is sample size). Modelling the aDNA data with the Stirling probability distribution suggested that the number of historical haplotypes was 43, with the lower 95% confidence interval being 28 (95% CI: 28-173, Fig. 3b).

402

403 The phylogenetic reconstruction of the combined historic (*n*=29) and modern data
404 (Haplotypes A-K) revealed three highly supported (>98% posterior probability) clades within
405 the woylie radiation (Fig. 4). These CR clades and haplotypes were also observed in the
406 cytochrome *b* phylogeny confirming topological consistency between mtDNA regions (Fig.
407 S2). Two historical haplotypes (samples MB816 and MB823) constituted a distinct clade,
408 which was not present within the extensively sampled modern populations, suggesting that
409 this particular clade is likely extinct. The other two clades consisted of an admixture of both
410 modern and historical haplotypes and spanned a broad geographical area.

411

412 Molecular clock analysis based on the cytochrome *b* dataset dated the most recent common
413 ancestor of the western Australian *B. penicillata* as living between 0.59 and 1.75 million years
414 ago (mean=1.2). This parameter was therefore included in the coalescent-based demographic
415 analysis of CR with a lognormal prior of mean 1,000,000 and SD=0.32 (in real space). Of the
416 three demographic models analysed, the BSP was the model with the best fit according to
417 differences in AICM estimates (constant population size: 2642.05, SE=0.08; exponential
418 growth: 2644.47, SE=0.08; BSP: 2572.52, SE=0.04). Based on this analysis, the woylie
419 population size for 2006-2008 was 99.86% lower than the historical population size (Fig. 5,
420 range: 99.3-99.97%). The mutation rate was estimated to be approximately 10% per million
421 years, placing the beginning of the population decline between ~4,600 and ~2,300 (95%
422 HPD) years ago.

423

424 The comparison of migration models with Migrate-n favoured the most complex model with
425 four distinct populations (LBF=5.9 with the next most likely model; Table 1), therefore we

summed the parameter values to obtain the species-wide demographic changes over time. Taking into account migration between populations, woylie numbers declined by a 89.1% compared to historical population size (Fig. 6a, range: 87.1-90.7).

Microsatellite data analysis

We implemented several quantitative and qualitative measures to improve the reliability of the microsatellite dataset. Following our strict approach, we only considered 21 historical samples, from which we obtained near-complete 11-loci microsatellite profiles (Table S1). From the PCR repetitions, we calculate a $P_{(fh)}$ for the locus Y112 of 36.4% and it was therefore excluded from all statistical comparisons. The remaining loci had lower $P_{(fh)}$ (range: 0-16.3%, Table 2). Hence, our protocol had less than 0.5% probability of falsely scoring an individual homozygous (except for the locus Y112, for which it was ~5%). Despite the limited number of historical individuals with full microsatellite profiles we observed nine individuals with at least one "unique allele" (i.e. alleles that were not present in modern data, Table 2). Levels of heterozygosity and average allelic richness (N_{AR}) varied across loci (Table 2) but were significantly higher in the historical dataset (N_{AR}: Wilcoxon tests: Z=-2.191, p=0.028; *IH*: Mann-Whitney test: Z=-2.45, p=0.014, Table 2, Fig. 3c). The three-parameter asymptotic exponential model was a marginally better fit (p=0.044) to the rarefaction data than the two-parameter model and predicted an expected mean number of alleles equal to 20.7 if 210 historical samples had been used (equation: $na = 20.74 - 0.88 \ e^{2.85 \ S}$, where *na* is expected number of alleles, and *S* is sample size). The numbers of migrants were consistently higher when compared with estimates calculated with the modern data alone (Table 3).

449 No evidence of a bottleneck was detected using the heterozygosity excess and the mode shift
450 analytical approaches. The M-ratio method, however, detected a reduction in population size
451 in all modern populations except for that from Perup, the eastern population in the Upper
452 Warren region.
453
454 Migrate-n strongly favoured a panmictic population (LBF>50,000 with the next most likely
455 model). Because the commencement of the decline is less clear in Migrate-n microsatellite
456 BSP (Fig. 6a), we calculated the extent of the decline from 2Θ because accuracy may
457 decrease beyond this point (P. Beerli personal communication) and detected a 56.5%
458 population decline in recent time.
459

460 ## Discussion

461 The aim of this study was to overlay data generated from historical samples on those from
462 extensively sampled modern populations (Pacioni *et al.* 2011), and evaluate whether
463 application of aDNA techniques enhances our understanding of the possible genetic impact of
464 declines in wildlife. Specifically, we set out to characterise ancient mitochondrial and
465 microsatellite DNA to address two key questions for conservation management, namely
466 quantifying the potential loss of genetic diversity and to assess the degree of former
467 connectivity between extant populations remaining within the species' highly fragmented
468 distribution. While modern data alone can be used to model past demographic events, it is not
469 as powerful as using direct measurements of genetic diversity based on ancient DNA. The
470 woylie exemplifies a common situation in that it is a critically endangered species where
471 genetics has been largely ignored in its management for the past 20 years, despite specific

recommendations in the woylie recovery plan (Start *et al.* 1995). This exclusion has prevented the establishment of management practices that seek to maximise the level of genetic diversity from amongst remaining populations. Lack of the genetic component also makes it impossible to evaluate whether assisted migration of individuals from different populations would be a viable management strategy.

Genetic diversity

The inclusion of aDNA data allowed us to conclude that the woylie underwent a dramatic genetic loss. This finding is somewhat in contrast with a previous assessment based only on modern data. In fact, modern levels of genetic diversity were considered relatively high (Pacioni *et al.* 2011). However, after the addition of data from historical samples, the rarefaction analysis and the estimation of the most likely number of haplotypes (n=43, 95% CI 28-173 Fig. 3b) confirmed a mtDNA genetic loss of ~65% (range: 46-91%, considering that only 15 haplotypes are still detectable in modern populations compared to a range of 28-173 expected historical haplotypes). These findings are also supported by comparisons of the historical and modern microsatellite data where we found a reduction of at least 20%.

The use of microsatellite loci in ancient DNA presents a challenge because of the potential problem of data fidelity associated with DNA degradation (Bourke *et al.* 2010; Morin *et al.* 2001). Amplification of microsatellite data from historical skins has been limited (Bourke *et al.* 2010), and even less frequent from fossil bones (Allentoft *et al.* 2014; Nyström *et al.* 2012). In our study, the inclusion of microsatellite data from historical samples proved to be very informative, demonstrating a significant reduction in allelic richness and heterozygosity across the loci examined. Furthermore, seven of the nine individuals with unique alleles were

from within or close to the woylie's current geographic distribution. Considering the large number of modern samples that were profiled (*n*=231, Pacioni *et al.* 2011), it is very likely that these alleles have been 'lost' from the modern populations. The three-parameter asymptotic exponential model predicted at least 20.7 historical alleles, suggesting a loss of at least 21.3%. Our results indicate how carefully one should interpret results based on modern data alone. In fact, based on the latter dataset, only limited concerns were raised on this aspect of woylie conservation (Pacioni *et al.* 2011), while this study clearly demonstrates a dramatic overall reduction in genetic diversity. Another example of the potential bias generated by the lack of baseline data, which can result in misleading management targets, is that the mean genetic diversity (from modern data) of the wild woylie populations considered in this study was used as a reference term to evaluate whether the genetic diversity of translocated populations was satisfactory (Pacioni *et al.* 2013). The characterisation of the historical genetic diversity, as conducted in this study, indicates that, while in principle that approach is valid, the conclusions are possibly rather optimistic.

It was only possible to quantify these estimations by including ancient DNA data and, considering the occurrence of allelic drop out that it is inevitable when working with aDNA, these should be considered conservative.

Demographic analyses

Data from historical samples also allowed a better understanding of the demographic history of the woylie compared with that obtained from modern samples only. Specifically, the historical data helped to quantify the extent of the decline and its consequences on the genetic diversity. Even with modern data alone, Migrate-n correctly detected the overall woylie

520 decline. However, in these analyses, the estimated historical population size was substantially
521 reduced as was the extent of the decline (Fig. 6). Differences in the results are even more
522 dramatic in BEAST analyses. In fact, when all historical samples for which we had time-
523 stamped data (*n*=22) were included in the mtDNA analysis, the 95% HPD intervals were
524 reduced and this analysis indicated that the woylie experienced more than a 99% decline in
525 population size in recent times. When this analysis was repeated including only modern data
526 (*n*=146, Fig. 5), it was not possible to discriminate between a constant population and a
527 declining trend in the demography of the woylie. Migrate-n analysis with microsatellite data
528 detected the decline even with modern data alone. However, in this analysis too, the
529 confidence intervals are slightly wider and the population size in recent times is mildly
530 underestimated. These results exemplify the potential problems in reconstructing past
531 demographic trajectories from modern data alone. It is evident that the inclusion of aDNA
532 data can be highly informative and it is likely to have important implications for the
533 management of threatened species.
534
535 The lack of significant results using common bottleneck tests highlights the limitations of
536 these methods. The M-ratio tests detected genetic bottleneck in three out of four remnant wild
537 populations, while the heterozygosity excess and mode-shift approaches did not detect a
538 bottleneck at all. Various factors can influence the statistical power of the bottleneck tests,
539 including the time since the bottleneck, the nature of the post-decline recovery and the
540 effective population size pre-bottleneck (Busch *et al.* 2007; Cornuet & Luikart 1996; Garza &
541 Williamson 2001; Williamson-Natesan 2005). We argue that the timing of the modern
542 population sampling was too close to or contemporary with the most recent declines (i.e. after
543 1999), for them to be detected (despite the substantial loss of genetic diversity) by the

544 heterozygosity excess and mode-shift methods (Cornuet & Luikart 1996; Garza &
545 Williamson 2001; Williamson-Natesan 2005). Possibly, the demographic post-reduction
546 growth, consequent upon the fox control programs started in the late 1990s, created a
547 heterozygosity deficiency, which balanced out the heterozygosity excess following the
548 bottleneck subsequent to the European settlement. On the other hand, we consider the results
549 of the M-ratio analyses indicating a genetic bottleneck to be the outcome of substantial
550 declines in the 20th century as opposed to the most recent declines. The M-ratio approach can
551 detect a bottleneck up to 100 generations post decline (Garza & Williamson 2001), which
552 would correspond to ~250 years in the woylie (Groom 2010; Pacioni 2010). This is also
553 supported by the observation that the new alleles found in historical samples were within the
554 allele frequency distributions of the modern populations (i.e. their loss is responsible for a
555 decrease of the M-ratio).
556
557 *Gene flow*
558 With the exception of the pair Kingston-Perup, the other modern populations are, nowadays,
559 completely isolated (Pacioni *et al.* 2011). The coalescent-based analyses, demonstrated that
560 historically these sites were connected, a finding that was only the subject of speculation in
561 Pacioni *et al*. (2011). Analysis of microsatellite data suggests that these were actually part of a
562 large panmictic population. These results are also supported by the private allele analysis,
563 despite the limitations of this approach mentioned above. In this analysis, the estimates of the
564 number of migrants between localities increased when data from the limited number of
565 historical samples were included. This demonstrates a wider spatial distribution of alleles, just
566 a hundred years ago (when most historical samples were collected), than that found at present.

567 It is intriguing to note that the last hundred years is a time consistent with the substantial
568 habitat loss and fragmentation in the WA Wheat-belt region (Saunders 1979).
569
570 The differences between the migration models supported by mtDNA and microsatellite data
571 are not surprising. In fact, woylies have a male-biased dispersal (Christensen 1980; Pacioni
572 2010), with females normally settling near to their mother's home range boundaries (Pacioni
573 2010). Males are, therefore, primarily responsible for long-distance gene flow, which is not
574 detected in the mtDNA data as mtDNA is maternally inherited.
575

576 *Timing of the decline*

577 We used BEAST to attempt to establish the time of commencement of the decline, because
578 BEAST can take into account uncertainty around the evolutionary rates and calibration points
579 while reconstructing the phylogeny and the demographic history. While our sampling regime
580 (which was mid way between the "pooled" and "scattered" sampling strategies) should not be
581 prone to substantial biases (Heller *et al.* 2013), we acknowledge a possible bias in the
582 inference of the demographic history in the BSP, because there is a strong indication of
583 reduced gene flow between different regions within Western Australia in recent times. Habitat
584 fragmentation and isolation of the studied populations generally lead to an underestimation of
585 population size (Heller *et al.* 2013), and consequently the extent of the demographic decline
586 may be overestimated. The effect of fragmentation on calculations of evolutionary rates is less
587 predictable. Contrary to expectations, when using the same input data in BEAST as for the
588 Migrate-n analysis (limiting data to samples geographically representative of the four modern
589 populations), BEAST estimation of historical population size appears to be more conservative
590 (although not substantially different), and the timing of the decline is only slightly shifted

toward the present (Fig. S3). It should be stressed that such estimates are subject to uncertainties because the inter-specific mutation rates are probably lower than the intra-specific rates (Ho *et al.* 2008) and, accordingly, caution the reader to interpret these results with care. We argue that, while it is difficult to pinpoint exactly when the decline commenced its downward trajectory, it is clear that it started recently (i.e. less than ~4,000 years ago) and has continued to the present. A possible catalyst for the start of this decline could have been the arrival of the dingo (*Canis lupus dingo*) in Australia (3,500-5,000 years ago, Fillios *et al.* 2012; Savolainen *et al.* 2004), but based on the observation of the substantial loss of genetic diversity compared to samples from as recently as 100 years ago, we also argue that the decline has been intensified since European settlement. Additional time-stamped samples that increase the time span covered by the aDNA data may help to more accurately estimate the timing of woylie decline, as it remains uncertain whether European factors (foxes, cats, disease), pre-European factors (e.g. dingo or fire regimes), or a combination of both, were the trigger for the decline in woylie genetic diversity and population numbers.

Implications for woylie conservation

The findings of this study have direct implications for the conservation and management of the critically endangered woylie in south-western Australia. Notably, evidence of a much wider former connectivity between the now fragmented habitats where the modern populations reside is highly relevant. Managing small isolated populations is challenging due to their susceptibility to stochastic events and greater effects of genetic drift (Frankham 1996; Frankham *et al.* 1999). Our findings show that there is a precedent for re-establishing gene flow between the currently isolated populations. Strategies such as natural corridors and

translocations could help restore gene flow to historical levels and assist in the maintenance of the remaining genetic diversity.

Through direct measurement of ancient genetic variability, we uncovered the extent of genetic diversity loss in the woylie that occurred along with a substantial demographic reduction. A very conservative estimate of genetic loss would be of 65% for mtDNA and 20% for nuclear DNA, but in reality the number is likely to be far greater given the rate at which new genetic variants were detected in the ancient gene pool. This loss of genetic diversity can be attributed directly to the massive population decline detected with the BSP analysis. The severity and tempo of the decline should act as a catalyst for more active management strategies that seek to maintain the existing species-wide genetic diversity. The translocated woylie populations that were established in the late 1980s (e.g. populations in South Australia, Delroy *et al.* 1986), despite being at lower genetic diversity than indigenous populations (Pacioni *et al.* 2013), may have captured some of the genetic diversity that it is now lost in Western Australia and may play a role in the future genetic management of the woylie. Indeed, a haplotype found in South Australian translocated populations was not found in Western Australian populations, but it was identified from an historical sample from Dryandra.

A further conservation outcome is the characterisation of woylie genetics at the boundaries of the species' distribution. For example, our profiling of fossil material from Faure Island, at the northern limit of the former distribution, demonstrated that the woylies that once inhabited this region were genetically very similar to extant populations despite being more than 1000 km away. Faure Island and Dirk Hartog Island are important sites in the Shark Bay World Heritage Area for ecosystem restoration (DEC 2005), which involves translocations of

638 previously present species to re-establish past biodiversity in the region. Our data suggest that
639 the use of the available genetic stock is appropriate and it is not unreasonable to expect that
640 woylies might adapt easily to these relatively more arid environments.
641

642 *Conclusion*

643 The mode and tempo of genetic diversity loss is often difficult to quantify in species that have
644 already undergone significant declines. The south-west of Western Australia is a biodiversity
645 hotspot and therefore a critical region for conservation purposes, yet baseline data for past
646 biodiversity are limited. Moreover, many marsupials are still in decline in Australia but it is
647 difficult to quantify changes in the genetic profile of these species over time. We set out to
648 investigate how knowledge of the past might assist best-practice conservation in the present.
649 The south-west of Western Australia used to provide a rich, continuous habitat to numerous,
650 now endangered species and while we focused on only one species, it is likely that the degree
651 of genetic diversity loss is directly relevant to many endemic species in the region. Whilst
652 detailed screening of available fossils and skins was conducted in the case of the woylie, the
653 number of samples available in these kinds of studies will always be limiting. The lack of
654 samples for key localities, sampling restrictions on skin and bone voucher specimens and
655 constraints imposed by DNA preservation are all limitations when trying to quantify past
656 diversity using ancient DNA techniques. Despite these limitations, this study demonstrates
657 that the inclusion of historical material in genetic studies is beneficial for wildlife
658 management and conservation. We demonstrated that the inclusion of aDNA data improves
659 the quantification of genetic diversity changes and inference of historical population
660 dynamics. Additionally, we advocate that, when technically feasible, it is important to expand
661 ancient DNA studies past the use of mtDNA in an attempt to quantify what has occurred at

662 the nuclear DNA level; both microsatellite data and SNPs (single nucleotide polymorphisms)
663 can provide these insights and such approaches are aided by next generation DNA sequencing
664 platforms. This becomes especially relevant in species where male-biased dispersal may skew
665 mtDNA interpretation of diversity, connectivity and phylogeography.
666

667 ## Acknowledgments

668 We thank the Wardandi people of south-western Australia for their support of the original
669 archaeological excavations that provided many of the samples analysed. Thanks to Ric How
670 and the WA museum for historical samples and assistance. Computer simulations were
671 supported by PAWSEY through the use of advanced computing resources provided by the
672 Informatics Facility located at Murdoch University and CIPRES
673 (http://www.phylo.org/sub_sections/portal/cite.php). We would like to thank Stefan Prost and
674 Christian Anderson for promptly integrating our suggestion of a 'pie chart' feature in
675 Tempnet. Simon Ho, Martyna Molak and Alexei Drummond provided useful comments
676 regarding analysis of aDNA data and two anonymous reviewers whose suggestions greatly
677 improved this manuscript. We are very grateful to Peter Beerli, who provided advice and
678 assistance in Migrate-n analyses. This research was funded by an ARC future fellowship
679 (MB) to explore past biodiversity in WA (FT0991741).
680

681 ## References

682 Allentoft ME, Collins M, Harker D*, et al.* (2012) The half-life of DNA in bone: measuring
683 decay kinetics in 158 dated fossils. *Proceedings of the Royal Society of London B:*
684 *Biological Sciences*, **279**, 4724-4733.
685 Allentoft ME, Heller R, Oskam CL*, et al.* (2014) Extinct New Zealand megafauna were not
686 in decline before human colonization. *Proceedings of the National Academy of*
687 *Sciences of the United States of America*, **111**, 4922-4927.

688 Allentoft ME, Oskam C, Houston J*, et al.* (2011) Profiling the dead: generating
689 microsatellite data from fossil bones of extinct megafauna—protocols, problems,
690 and prospects. *PLoS One*, **6**, e16670.
691 Andrén H (1994) Effects of habitat fragmentation on birds and mammals in landscapes
692 with different proportions of suitable habitat: a review. *Oikos*, **71**, 355-366.
693 Baele G, Li WLS, Drummond AJ, Suchard MA, Lemey P (2012) Accurate model selection
694 of relaxed molecular clocks in Bayesian phylogenetics. *Molecular Biology and*
695 *Evolution*, **30**, 239-243.
696 Barton NH, Slatkin M (1986) A quasi-equilibrium theory of the distribution of rare
697 alleles in a subdivided population. *Heredity*, **56**, 409-415.
698 Beerli P (2006) Comparison of Bayesian and maximum-likelihood inference of
699 population genetic parameters. *Bioinformatics*, **22**, 341-345.
700 Bourke BP, Frantz AC, Lavers CP*, et al.* (2010) Genetic signatures of population change in
701 the British golden eagle (Aquila chrysaetos). *Conservation Genetics*, **11**, 1837-
702 1846.
703 Bouzat JL, Paige KN, Lewin HA (1998) The ghost of genetic diversity past: historical DNA
704 analysis of the greater prairie chicken. *The American Naturalist*, **152**, 1-6.
705 Brace S, Palkopoulou E, Dalén L*, et al.* (2012) Serial population extinctions in a small
706 mammal indicate Late Pleistocene ecosystem instability. *Proceedings of the*
707 *National Academy of Sciences of the United States of America*, **109**, 20532-20536.
708 Briggs AW, Stenzel U, Johnson PLF*, et al.* (2007) Patterns of damage in genomic DNA
709 sequences from a Neandertal. *Proceedings of the National Academy of Sciences of*
710 *the United States of America*, **104**, 14616-14621.
711 Burbidge AA, Johnson KA, Fuller PJ, Southgate RI (1988) Aboriginal knowledge of the
712 mammals of the central deserts of Australia. Australian *Wildlife Research*, **15**, 9-
713 39.
714 Burbidge AA, McKenzie NL (1989) Patterns in the modern decline of Western Australia's
715 vertebrate fauna: causes and conservation implications. *Biological Conservation*,
716 **50**, 143-198.
717 Busch JD, Waser PM, DeWoody JA (2007) Recent demographic bottlenecks are not
718 accompanied by a genetic signature in banner-tailed kangaroo rats (*Dipodomys*
719 *spectabilis*). *Molecular Ecology*, **16**, 2450-2462.
720 Campos PF, Willerslev E, Sher A*, et al.* (2010) Ancient DNA analyses exclude humans as
721 the driving force behind late Pleistocene musk ox (Ovibos moschatus) population
722 dynamics. *Proceedings of the National Academy of Sciences of the United States of*
723 *America*, **107**, 5675-5680.
724 Christensen PES (1980) *The biology of Bettongia penicillata Gray, 1837, and Macropus*
725 *eugenii (Desmarest, 1817) in relation to fire.* Forests Deptment of Western
726 Australia Bulletin, No. 91, i-ix, 1-90, Perth.
727 Cornuet JM, Luikart G (1996) Description and power analysis of two tests for detecting
728 recent population bottlenecks from allele frequency data. *Genetics*, **144**, 2001-
729 2014.
730 DEC (2005) *Shark Bay terrestrial reserves and proposed terrestrial reserve additions*
731 *management plan.* Department of Environment and Conservation.
732 Delroy LB, Earl J, Radbone I, Robinson AC, Hewett M (1986) The breeding and re-
733 establishment of the brush-tailed bettong, *Bettongia penicillata*, in South-
734 Australia. Australian *Wildlife Research*, **13**, 387-396.

735 Dixon CJ (2006) A means of estimating the completeness of haplotype sampling using
736 the Stirling probability distribution. *Molecular Ecology Notes*, **6**, 650-652.
737 Dortch J (2004a) Late Quaternary vegetation change and the extinction of Black-flanked
738 Rock-wallaby (Petrogale lateralis) at Tunnel Cave, southwestern Australia.
739 *Palaeogeography, Palaeoclimatology, Palaeoecology*, **211**, 185-204.
740 Dortch J (2004b) *Paleo-environmental change and the persistence of human occupation in*
741 *south-western Australian forests.* British Archaeological Reports, International
742 Series 1288.
743 Drummond A, Rambaut A (2007) BEAST: Bayesian evolutionary analysis by sampling
744 trees. *BMC Evolutionary Biology*, **7**, 214.
745 Drummond AJ, Suchard MA, Xie D, Rambaut A (2012) Bayesian phylogenetics with
746 BEAUti and the BEAST 1.7. *Molecular Biology and Evolution*, **29**, 1969-1973.
747 Ewers RM, Didham RK (2006) Confounding factors in the detection of species responses
748 to habitat fragmentation. *Biological Reviews*, **81**, 117-142.
749 Fillios M, Crowther MS, Letnic M (2012) The impact of the dingo on the thylacine in
750 Holocene Australia. *World Archaeology*, **44**, 118-134.
751 Frankham R (1995) Effective population size/adult population size ratios in wildlife: a
752 review. *Genetics Research*, **66**, 95-107.
753 Frankham R (1996) Relationship of genetic variation to population size in wildlife.
754 *Conservation Biology*, **10**, 1500-1508.
755 Frankham R, Ballou JD, Briscoe DA (2002) *Introduction to conservation genetics.*
756 Cambridge University Press, Cambridge.
757 Frankham R, Lees K, Montgomery ME*, et al.* (1999) Do population size bottlenecks
758 reduce evolutionary potential? *Animal Conservation*, **2**, 255-260.
759 Gagneux P, Boesch C, Woodruff DS (1997) Microsatellite scoring errors associated with
760 noninvasive genotyping based on nuclear DNA amplified from shed hair.
761 *Molecular Ecology*, **6**, 861-868.
762 Garza JC, Williamson EG (2001) Detection of reduction in population size using data
763 from microsatellite loci. *Molecular Ecology*, **10**, 305-318.
764 Gilbert MTP, Bandelt H-J, Hofreiter M, Barnes I (2005) Assessing ancient DNA studies.
765 *Trends in Ecology & Evolution*, **20**, 541-544.
766 Groom C (2010) Justification for continued conservation efforts following the delisting
767 of a threatened species: a case study of the woylie, *Bettongia penicillata ogilbyi*
768 (Marsupialia: Potoroidae). *Wildlife Research*, **37**, 183-193.
769 Heller R, Chikhi L, Siegismund HR (2013) The confounding effect of population structure
770 on Bayesian skyline plot inferences of demographic history. *PLoS One*, **8**, e62992.
771 Ho SY, Saarma U, Barnett R, Haile J, Shapiro B (2008) The effect of inappropriate
772 calibration: three case studies in molecular ecology. *PLoS One*, **3**, e1615.
773 Ho SYW, Shapiro B (2011) Skyline-plot methods for estimating demographic history
774 from nucleotide sequences. *Molecular Ecology Resources*, **11**, 423-434.
775 Hunt H (2010) *A temporal assessment investigating the effects of population declines on*
776 *genetic diversity, in the critically endangered woylie (Bettongia penicillata ogilbyi).*
777 Honours thesis, Murdoch University.
778 Kalinowski ST (2004) Counting alleles with rarefaction: private alleles and hierarchical
779 sampling designs. *Conservation Genetics*, **5**, 539-543.

780 Kalinowski ST (2006) hw-quickcheck: an easy-to-use computer program for checking
781 genotypes for agreement with Hardy-Weinberg expectations. *Molecular Ecology*
782 *Notes*, **6**, 974-979.
783 Leonard JA (2008) Ancient DNA applications for wildlife conservation. *Molecular*
784 *Ecology*, **17**, 4186-4196.
785 Librado P, Rozas J (2009) DnaSP v5: a software for comprehensive analysis of DNA
786 polymorphism data. *Bioinformatics*, **25**, 1451-1452.
787 Luikart G, Cornuet JM (1998) Empirical evaluation of a test for identifying recently
788 bottlenecked populations from allele frequency data. *Conservation Biology*, **12**,
789 228-237.
790 Morin P, Chambers K, Boesch C, Vigilant L (2001) Quantitative polymerase chain
791 reaction analysis of DNA from noninvasive samples for accurate microsatellite
792 genotyping of wild chimpanzees (Pan troglodytes verus). *Molecular Ecology*, **10**,
793 1835-1844.
794 Myers N, Mittermeier RA, Mittermeier CG, da Fonseca GAB, Kent J (2000) Biodiversity
795 hotspots for conservation priorities. *Nature*, **403**, 853-858.
796 Navascués M, Depaulis F, Emerson BC (2010) Combining contemporary and ancient
797 DNA in population genetic and phylogeographical studies. *Molecular Ecology*
798 *Resources*, **10**, 760-772.
799 Neal RM (2003) Slice sampling. *Annals of statistics*, **31**, 705-741.
800 Nei M (1987) *Molecular evolutionary genetics.* Columbia University Press, New York.
801 Nyström V, Humphrey J, Skoglund P*, et al.* (2012) Microsatellite genotyping reveals end
802 Pleistocene decline in mammoth autosomal genetic variation. *Molecular Ecology*,
803 **21**, 3391-3402.
804 Oksanen J, Blanchet GF, Kindt R*, et al.* (2013) Vegan: Community Ecology Package. R
805 package version 2.0-8.
806 Pacioni C (2010) *The population and epidemiological dynamics associated with recent*
807 *decline of woylies (Bettongia penicillata) in Australia.* PhD, Murdoch University.
808 Pacioni C, Spencer P (2010) Capturing genetic information using non-target species
809 markers in a species that has undergone a population crash. *Australian*
810 *Mammalogy*, **32**, 33-38.
811 Pacioni C, Wayne AF, Spencer P (2013) Genetic outcomes from the translocations of the
812 critically endangered woylie. *Current Zoology*, **59**, 294-310.
813 Pacioni C, Wayne AF, Spencer PBS (2011) Effects of habitat fragmentation on population
814 structure and long distance gene flow in an endangered marsupial: the woylie.
815 *Journal of Zoology*, **283**, 98-107.
816 Peakall ROD, Smouse PE (2006) GENALEX 6: genetic analysis in Excel. Population
817 genetic software for teaching and research. *Molecular Ecology Notes*, **6**, 288-295.
818 Peery MZ, Kirby R, Reid BN*, et al.* (2012) Reliability of genetic bottleneck tests for
819 detecting recent population declines. *Molecular Ecology*, **21**, 3403-3418.
820 Piry S, Luikart G, Cornuet JM (1999) Computer note. BOTTLENECK: a computer program
821 for detecting recent reductions in the effective population size using allele
822 frequency data. *Journal of Heredity*, **90**, 502-503.
823 Posada D, Crandall KA (1998) MODELTEST: testing the model of DNA substitution.
824 *Bioinformatics*, **14**, 817-818.

825 Prost S, Anderson CNK (2011) TempNet: a method to display statistical parsimony
826 networks for heterochronous DNA sequence data. *Methods in Ecology and*
827 *Evolution*, **2**, 663-667.
828 R DevelopmentCore Team (2015) R: A language and environment for statistical
829 computing. R Foundation for statistical computing, Vienna, Austria. ISBN 3-
830 900051-07-0, Vienna.
831 Ramakrishnan UMA, Hadly EA (2009) Using phylochronology to reveal cryptic
832 population histories: review and synthesis of 29 ancient DNA studies. *Molecular*
833 *Ecology*, **18**, 1310-1330.
834 Rambaut A, Drummond AJ (2007) TRACER. http://beast.bio.ed.ac.uk/Tracer
835 Rioux Paquette S (2011) PopGenKit: useful functions for (batch) file conversion and data
836 resampling in microsatellite datasets. R package, version 1.0.
837 Rousset F (2008) GENEPOP'007: a complete re-implementation of the GENEPOP
838 software for Windows and Linux. *Molecular Ecology Resources*, **8**, 103-106.
839 Saunders D (1979) The availability of tree hollows for use as nest sites by White-tailed
840 Black Cockatoos. Australian *Wildlife Research*, **6**, 205-216.
841 Savolainen P, Leitner T, Wilton AN, Matisoo-Smith E, Lundeberg J (2004) A detailed
842 picture of the origin of the Australian dingo, obtained from the study of
843 mitochondrial DNA. *Proceedings of the National Academy of Sciences of the United*
844 *States of America*, **101**, 12387-12390.
845 Shapiro B, Drummond AJ, Rambaut A*, et al.* (2004) Rise and fall of the Beringian steppe
846 bison. *Science*, **306**, 1561-1565.
847 Start AN, Burbidge AA, Armstrong D (1998) A review of the conservation status of the
848 woylie, *Bettongia penicillata ogilbyi* (Marsupialia: Potoroidae) using IUCN
849 criteria. *CalmScience*, **2**, 277-289.
850 Start T, Burbidge AA, Armstrong D, Woylie Recovery Team (1995) *Woylie recovery plan*,
851 2nd edn. Department of Conservation and Land Management, Como.
852 Taylor AC, Sherwin WB, Wayne RK (1994) Genetic variation of microsatellite loci in a
853 bottlenecked species: the northern hairy-nosed wombat Lasiorhinus krefftii.
854 *Molecular Ecology*, **3**, 277-290.
855 Van Dyck S, Strahan R (2008) *The mammals of Australia*, 3rd edn. New Holland
856 Publishers, Sydney.
857 Wayne AF, Friend T, Burbidge AA, Morris K, Van Weenen J (2008a) *Bettongia penicillata*
858 www.iucnredlist.org
859 Wayne AF, Maxwell M, Ward C*, et al.* (2013) The importance of getting the numbers
860 right: quantifying the rapid and substantial decline of an abundant marsupial,
861 *Bettongia penicillata*. *Wildlife Research*, **40**, 169-183.
862 Wayne AF, Maxwell M, Ward C*, et al.* (2015) Suddenand rapid decline of the abundant
863 marsupial *Bettongia penicillata* in Australia. *Oryx*, **49**, 175-185.
864 Wayne AF, Ward C, Maxwell M*, et al.* (2008b) Diagnosing the recent collapse of the
865 woylie in southwestern Australia, 21st Australian Wildlife Management Society
866 Conference, p.140.
867 Westerman M, Loke S, Springer MS (2004) Molecular phylogenetic relationships of two
868 extinct potoroid marsupials, *Potorous platyops* and *Caloprymnus campestris*
869 (Potoroinae: Marsupialia). *Molecular Phylogenetics and Evolution*, **31**, 476-485.
870 Willerslev E, Cooper A (2005) Review paper. ancient dna. *Proceedings of the Royal*
871 *Society of London B: Biological Sciences*, **272**, 3-16.

Williamson-Natesan EG (2005) Comparison of methods for detecting bottlenecks from microsatellite loci. *Conservation Genetics*, **6**, 551-562.
Woinarski JCZ, Burbidge AA, Harrison PL (2015) Ongoing unraveling of a continental fauna: Decline and extinction of Australian mammals since European settlement. *Proceedings of the National Academy of Sciences of the United States of America*, **112**, 4531-4540.

Data Accessibility:

DNA sequences: Genbank accession numbers KT876917-KT876973

Microsatellite data, and BEAST and Migrate-n input and parameter files: Dryad Digital Repository: doi:10.5061/dryad.26s85

Author contributions:

CP and MB conceived the experiments. AW, AB and JD assisted with sample selection, dating and conservation implications. CP, HH, MA, DH and TV generated and analysed the data and prepared figures/tables. CP, HH, MA and MB wrote the paper with input from all co-authors.

892

893 Figure Legends

894 **Fig. 1.** Localities of historical woylie fossil and museum specimens sampled in south-west
895 Western Australia (WRS: Witchcliffe Rock Shelter). Modern populations are indicated in
896 capital letters within grey squares: UW=Upper Warren, D=Dryandra, T=Tutanning). Grey
897 area in the insert: former *Bettongia penicillata* distribution including both subspecies
898 *Bettongia penicillata ogilbyi* and *B. p. penicillata* (adapted from Wayne *et al.* 2008b) based
899 on contemporary, fossils and Aboriginal knowledge records (Burbidge *et al.* 1988). Images of
900 the woylie (*B. p. ogilbyi*: (a) an adult woylie fitted with a VHF radio collar (Photo: John
901 Lawson), (b) skin and (c) fossil bone remains).

902

903 **Fig. 2.** Multidimensional parsimony network of mtDNA sequences from historical and
904 modern woylie samples (after removal of sequences with ambiguities). Dimensions of the
905 circles are proportional to the number of sequences for each haplotype. Margaret River is a
906 region that includes samples from WRS, Mammoth Cave and Tunnel Cave.

907

908 **Fig. 3.** a. and c. Rarefaction curves of modern and historical woylie data for (mtDNA)
909 haplotype richness and (microsatellite) allelic richness, respectively. Error bars indicate SE
910 from re-sampling iterations. b. Posterior probability distribution for expected total number of
911 haplotypes based on observed number of haplotypes and sampling effort in the historical
912 dataset.

913

Fig. 4. Bayesian phylogeny of *Bettoniga penicillata ogilbyi,* showing the maximum *a posteriori* (MAP) tree generated using BEAST. A GTR+G+I substitution model was imposed on an alignment containing the 29 historical CR sequences (~400bp) and 15 modern haplotype sequences (identified with an *) from Pacioni *et al.* (2011) detected in 152 modern samples (~600bp). Posterior probabilities are shown on the selected outer nodes. The scale represents the number of nucleotide substitutions per site. Three distinct clades are indicated on the tree. The tree topology is mirrored at the cytochrome *b* locus (see Fig. S2).

Fig. 5. Reconstruction of the woylie (*B. penicillata ogilbyi*) demographic history based on control region of mtDNA using a Bayesian Skyline Plot analysis implemented in BEAST v1.8 (Drummond *et al.* 2012). Shaded areas represent 95% Highest Probability Density (HPD). Solid lines represent the medians. Population size is expressed as log of the effective population size times the generation times.

Fig. 6. Reconstruction of the woylie (*B. penicillata ogilbyi*) demographic history based on control region of mtDNA (a) and microsatellite data (b) using a Bayesian Skyline Plot analysis implemented in Migrate-n v3.6.8 (Beerli 2006). In red analysis with modern data alone and in blue analysis including modern and ancient DNA data. Shaded areas represent 1.96 standard deviations from parameter values.

.

Tables

Table 1. Mode (2.5 and 97.5 percentile) of number of migrants between woylie populations (from row to column)

	Kingston	Perup	Tutanning	Dryandra
Kingston		1.1 (0-6.1)	n/a	4.8 (0-23.5)
Perup	0.3 (0.1-0.5)		n/a	5.1 (0-23.5)
Tutanning	n/a	n/a		0.1 (0-12.9)
Dryandra	0.1 (0.002-0.5)	2 (0.2-6.8)	0.5 (0-10.3)	

Table 2. Descriptive statistics of genetic diversity of microsatellite loci in the woylie (*Bettongia penicillata ogilbyi*) for modern (*n*=231)/historical (*n*=21) datasets. Between brackets SE.

Locus	H_o (%)	N_A	N_{AR}	U_A	$P_{(fh)}$
Bt76	85.3/85.7	19/14	10.5/11.57	2	2.2
Bt64	73.8/100	24/19	11.08/14.29	2	9.4
T17-2	68.7/90.5	16/14	10.07/11.13	1	6.5
Y175	82.2/78.9	19/13	10.57/10.5	0	14.3
Pa593	83.5/88.9	16/13	10.36/11.27	1	8
Y105	40.9/23.1	11/5	5.4/4.4	0	0
Y112*	73.7/90	29/11	12.46/11	1	36.4
Pl2	70.6/68.8	10/8	6.69/6.82	1	5.8
Y170	81/90	18/14	10.51/11.56	0	16.3
Bt80	76.9/58.3	12/10	7.92/9.54	1	8.5
Pl26	42.1/54.5	5/4	3.46/4	0	0
Mean	70.8(0.5)/75.3(0.7)	16.3(2.0)/11.4(1.3)	9.0(0.8)/9.6(1)	0.8(0.2)	9.8(3)

H_o, observed heterozygosity; N_A, number of alleles; N_{AR}, allelic richness; U_A, historical unique alleles; $P_{(fh)}$, frequencies of falsely scoring an individual as homozygous (%).

* Excluded from statistical tests because of evidence of substantial allelic dropout

Table 3. Number of migrants per generation between localities where modern woylie populations are located, calculated with the private allele method using 11 microsatellite loci (bold: ancient and modern DNA data, normal font: modern DNA data alone).

	Upper Warren	Tutanning	Dryandra
Upper Warren		0.52	0.91
Tutanning	**0.69**		0.68
Dryandra	**1.25**	**0.73**	

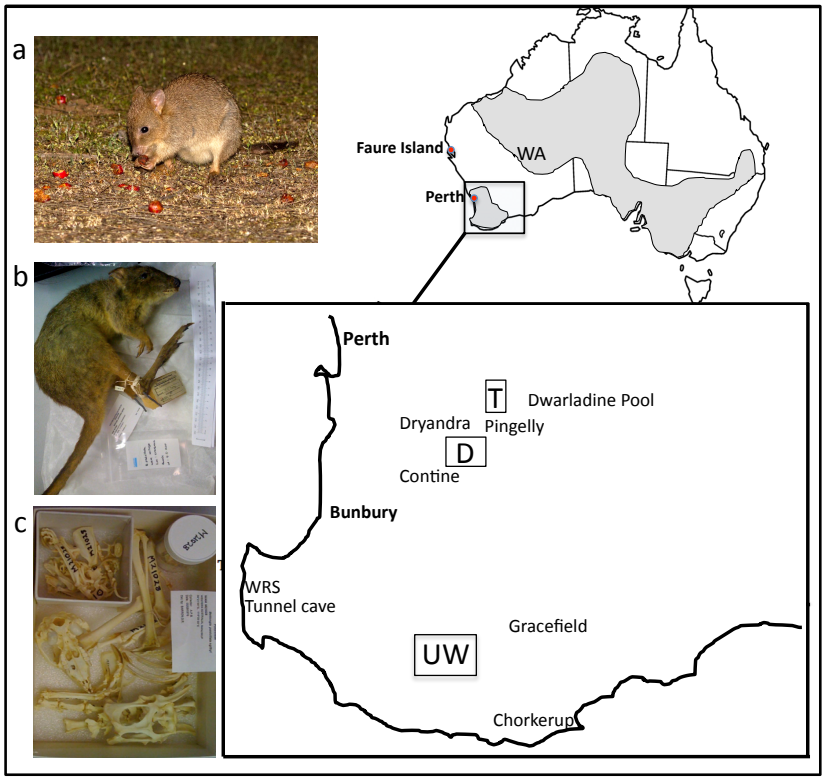
a
b
c
Faure Island
WA
Perth
Perth
T
Dwarladine Pool
Dryandra
Pingelly
D
Contine
Bunbury
WRS
Tunnel cave
Gracefield
UW
Chorkerup

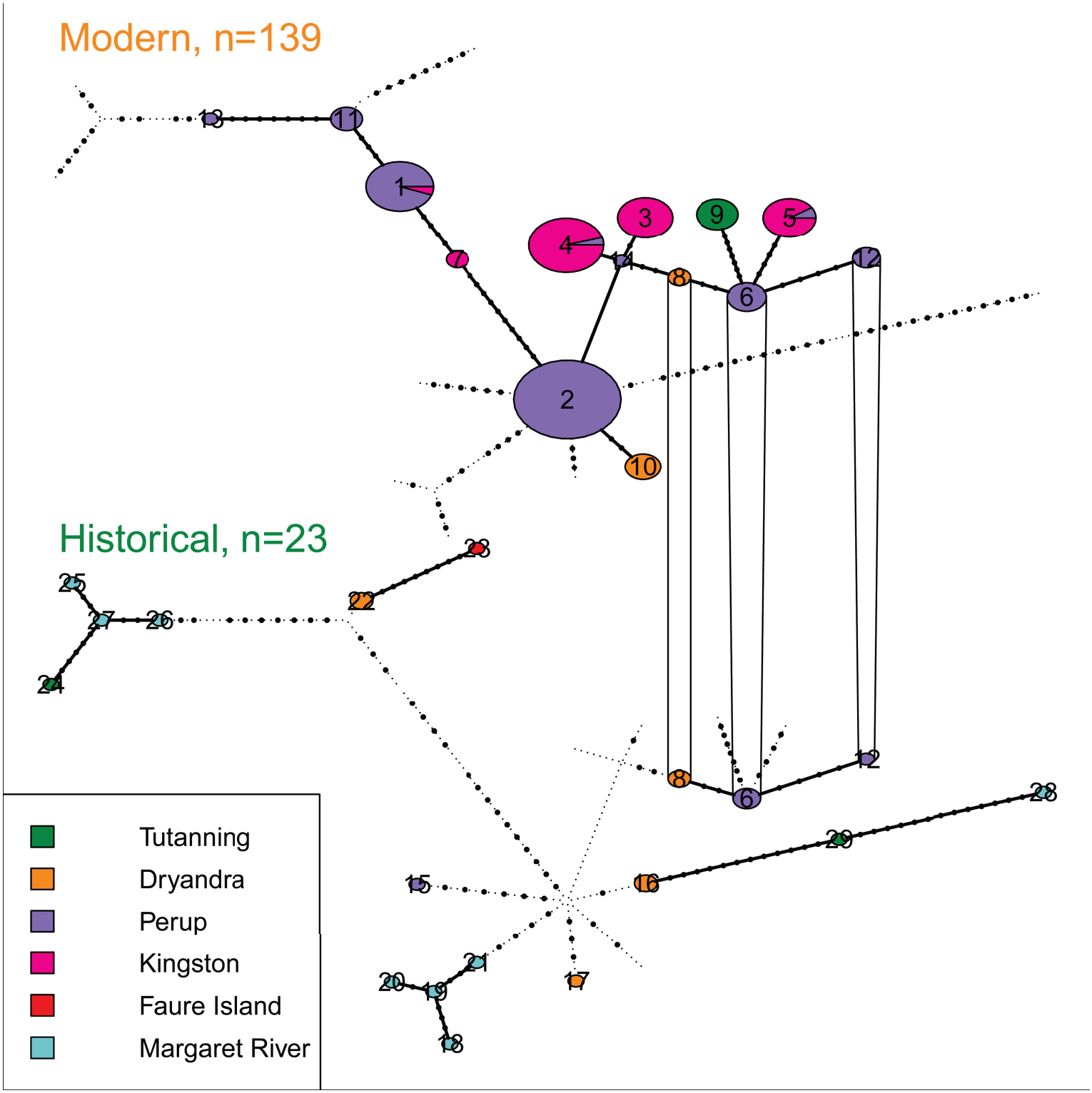
Modern, n=139
Historical, n=23
Tutanning
Dryandra
Perup
Kingston
Faure Island
Margaret River

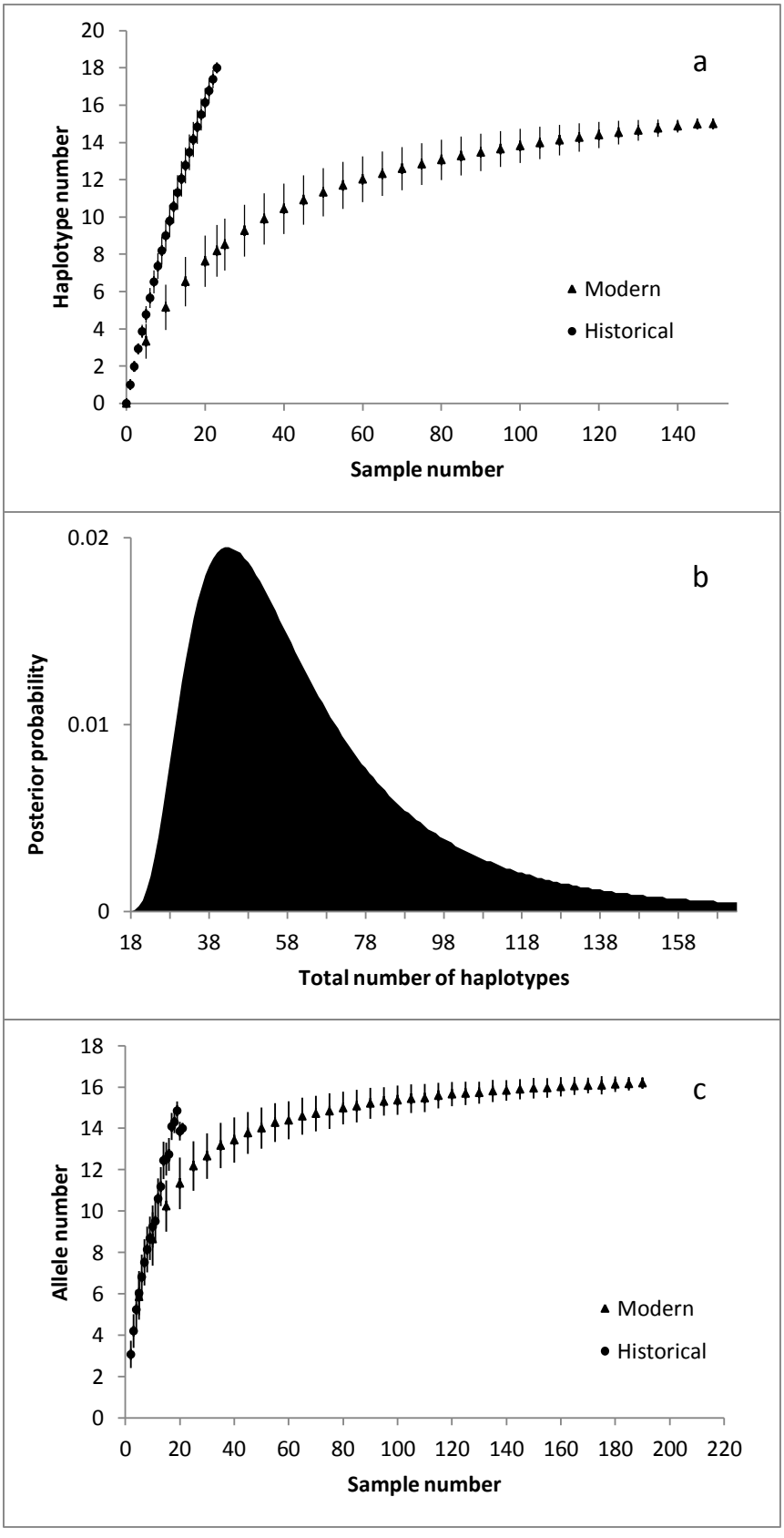
a
Haplotype number
Sample number
Modern
Historical
b
Posterior probability
Total number of haplotypes
c
Allele number
Sample number
Modern
Historical

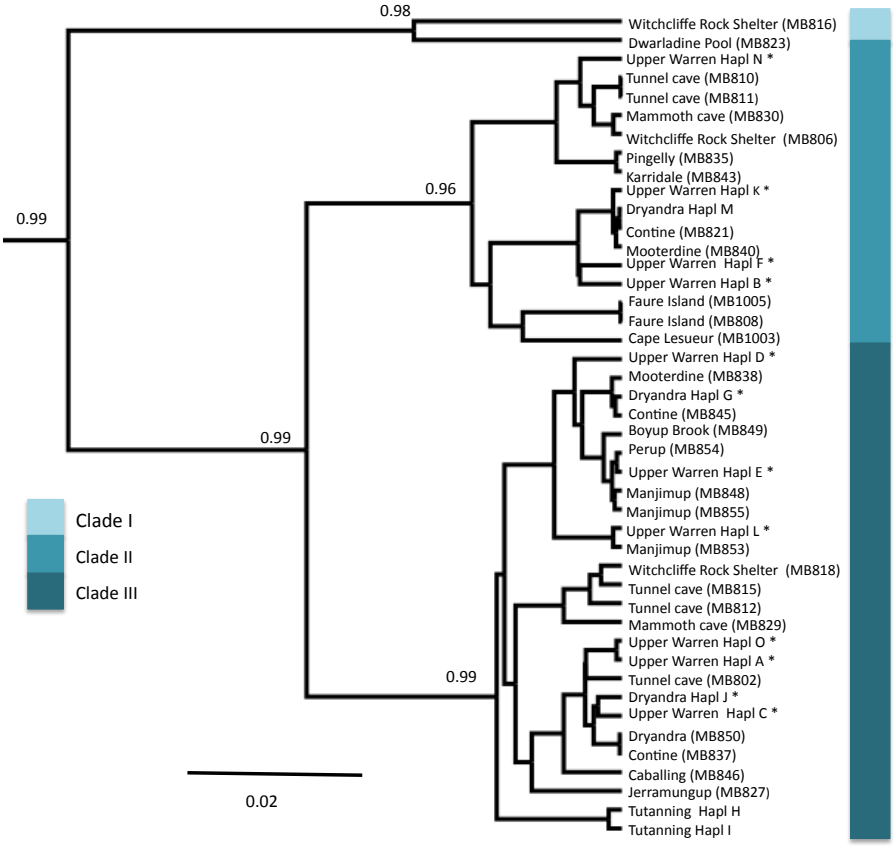
0.98
0.99
0.96
0.99
0.99
0.02
Witchcliffe Rock Shelter (MB816)
Dwarladine Pool (MB823)
Upper Warren Hapl N *
Tunnel cave (MB810)
Tunnel cave (MB811)
Mammoth cave (MB830)
Witchcliffe Rock Shelter (MB806)
Pingelly (MB835)
Karridale (MB843)
Upper Warren Hapl K *
Dryandra Hapl M
Contine (MB821)
Mooterdine (MB840)
Upper Warren Hapl F *
Upper Warren Hapl B *
Faure Island (MB1005)
Faure Island (MB808)
Cape Lesueur (MB1003)
Upper Warren Hapl D *
Mooterdine (MB838)
Dryandra Hapl G *
Contine (MB845)
Boyup Brook (MB849)
Perup (MB854)
Upper Warren Hapl E *
Manjimup (MB848)
Manjimup (MB855)
Upper Warren Hapl L *
Manjimup (MB853)
Witchcliffe Rock Shelter (MB818)
Tunnel cave (MB815)
Tunnel cave (MB812)
Mammoth cave (MB829)
Upper Warren Hapl O *
Upper Warren Hapl A *
Tunnel cave (MB802)
Dryandra Hapl J *
Upper Warren Hapl C *
Dryandra (MB850)
Contine (MB837)
Caballing (MB846)
Jerramungup (MB827)
Tutanning Hapl H
Tutanning Hapl I
Clade I
Clade II
Clade III

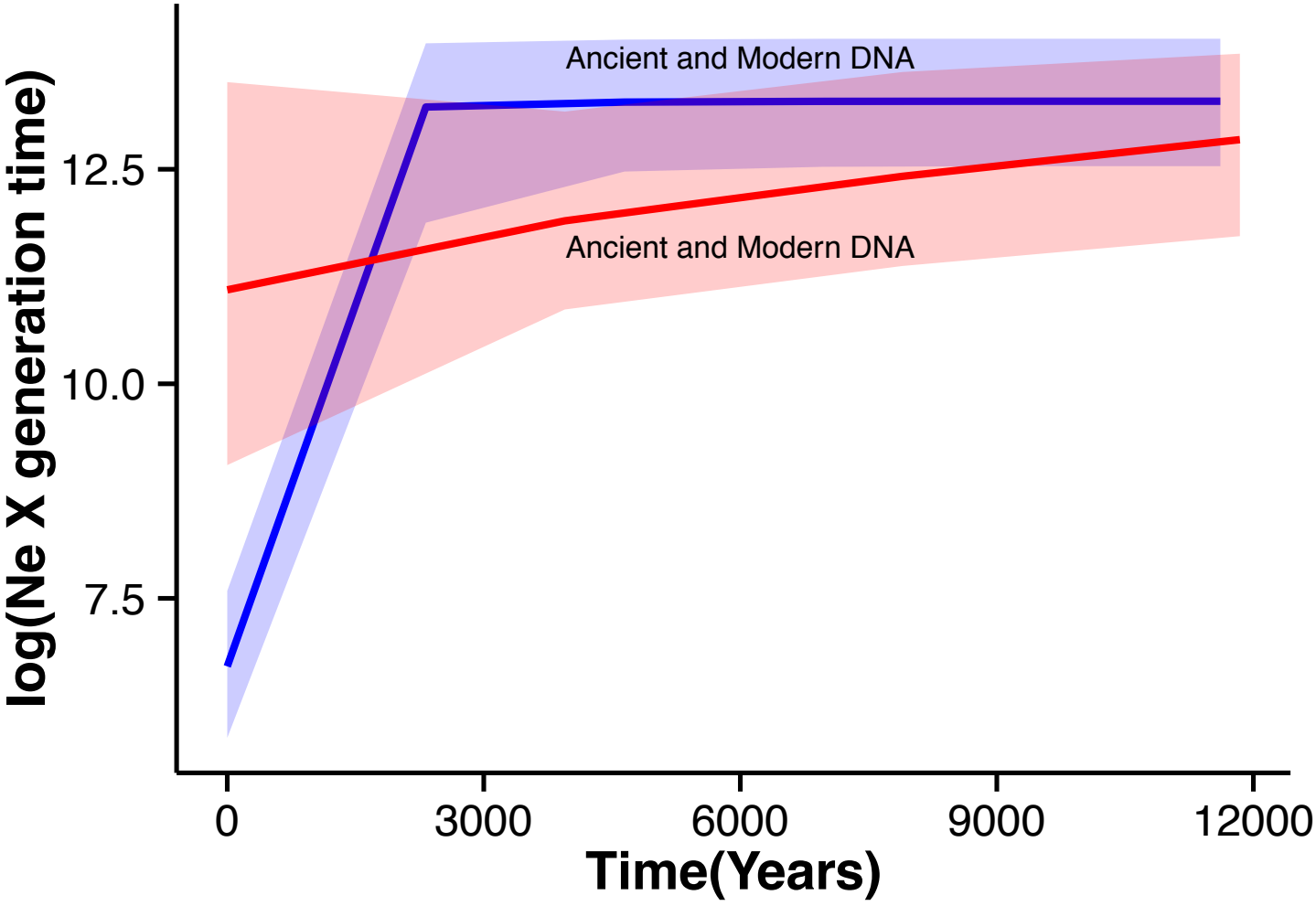
Ancient and Modern DNA
Ancient and Modern DNA
log(Ne X generation time)
12.5
10.0
7.5
0
3000
6000
9000
12000
Time(Years)

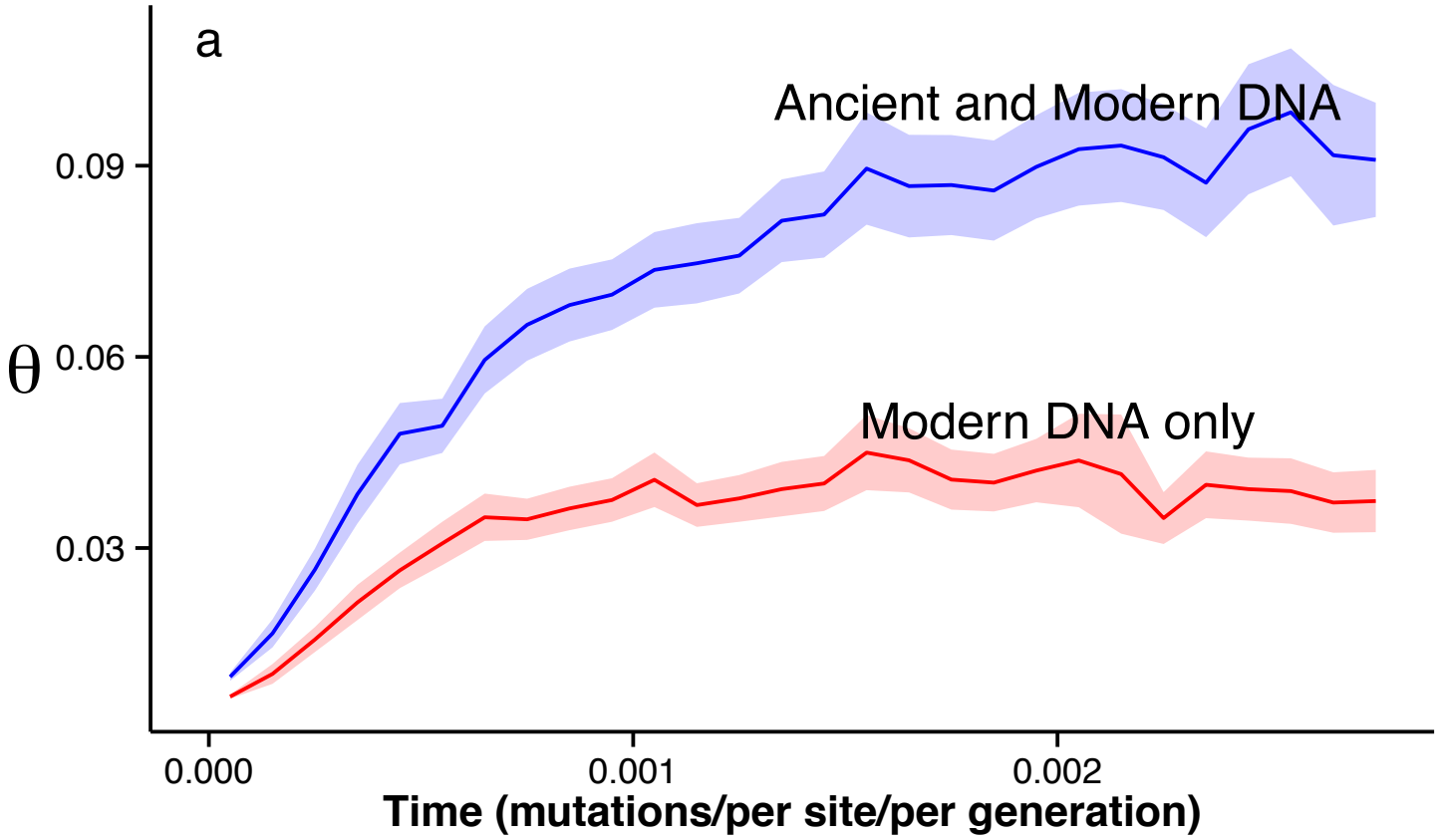
a
Ancient and Modern DNA
Modern DNA only
θ
0.09
0.06
0.03
0.000
0.001
0.002
Time (mutations/per site/per generation)

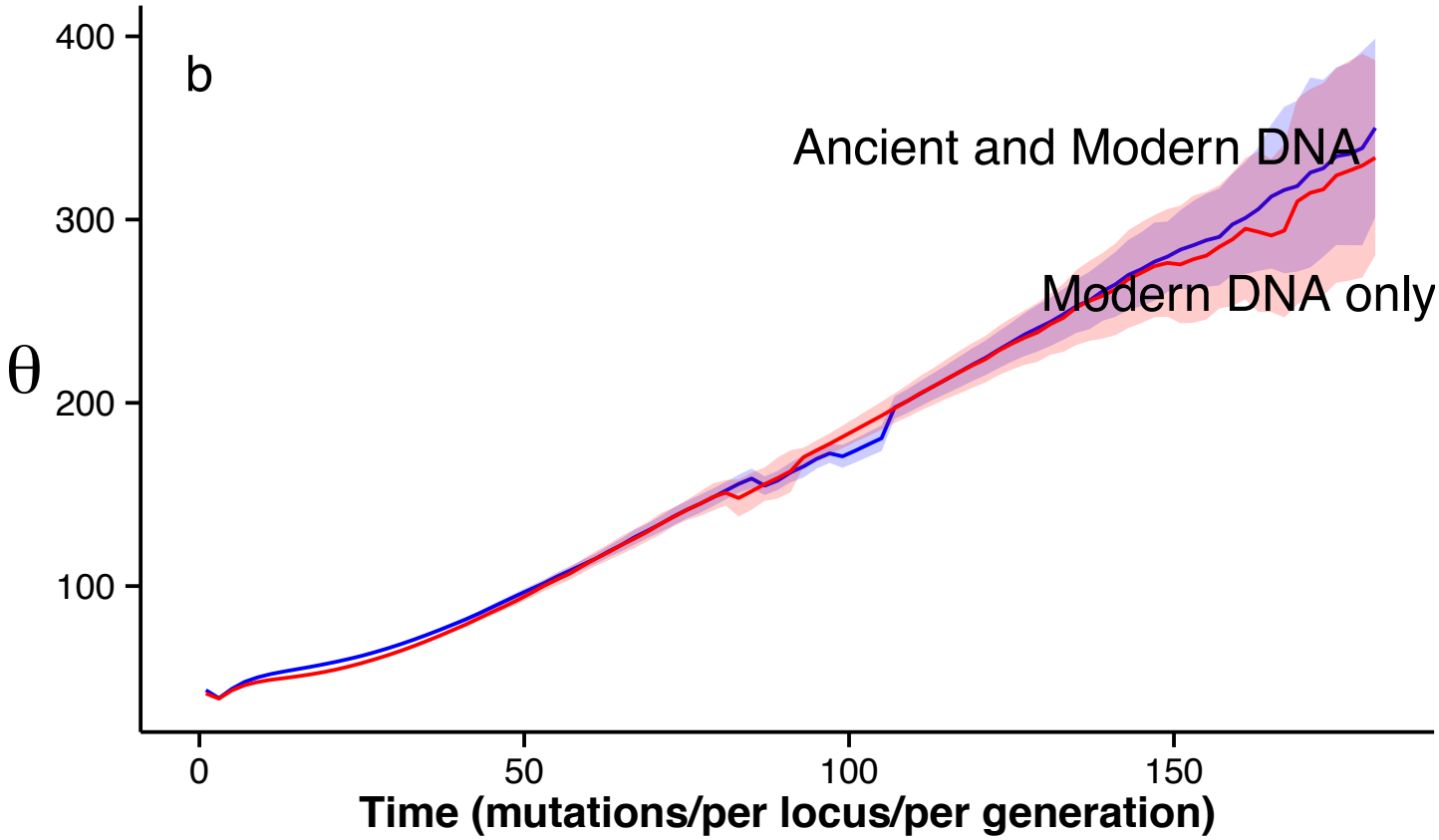
b
Ancient and Modern DNA
Modern DNA only
θ
400
300
200
100
0
50
100
150
Time (mutations/per locus/per generation)

Table S1. Summary of information of historical woylie *(Bettongia penicillata ogilbyi*) samples, including DNA preservation, age, and their use for statistical analyses.

Sample ID	C^{14} lab codes	Location	Uncalibrate Age (C^{14} error)	Age (year*)	Sample	Ct value	Largest Amplicon	Msat typed	BEAST BSP	Migrate-n BSP (mtDNA)	Migrate-n BSP (msats)
153		Faure Island		n/a	Bone	29.38	293				
173		Tunnel Cave	12840 (90)	15300 (14990-15570)	Bone	26.65	253				
187		Beaufort		108	Skin	25.79	253				
191		Pingelly		102	Bone	34.43	253				
190		Jerramungup		41	Skin	20.97	293				
794		Jerramungup		41	Skin	23.9	293	10			√
808		Faure Island		n/a	Bone	30.43	293	4			
802	Wk 4517	Tunnel Cave	12840 (90)	15300 (14990-15570)	Bone	34.3	253				
803	Wk 5474	Tunnel Cave	12890 (250)	15600 (14981-16262)	Bone	28.18	253				
810	Wk 4516	Tunnel Cave	4280 (60)	4800 (4739-4939)	Bone	35.74	253		√		
804	Wk 3625	Tunnel Cave	8270 (80)	9300 (9139-9384)	Bone	-	-				
805	Wk 6706, Wk 6707	Tunnel Cave	9860 (95)	11400 (11107-11666)	Bone	-	-				
811	Wk 4517	Tunnel Cave	12840 (90)	15300 (14990-15570)	Bone	-	253				
812	Wk 3626	Tunnel Cave	1370 (40)	1300 (1278-1322)	Bone	23.48	293	4	√		
813	Wk 3626, Wk 4516	Tunnel Cave	1370-4280 (40-60)†	3100 (1278-4939)	Bone	-	-				
814	Wk 4517	Tunnel Cave	12840 (90)	15300 (14990-15570)	Bone	29.61	253				
815	Wk 3626	Tunnel Cave	1370 (40)	1300 (1278-1322)	Bone	23.09	293	6	√		
816	Wk 3954, Wk 3955	Witchcliffe Rock Shelter	400-680 (50-90)†	500 (352-706)	Bone	36.39	293		√		
806	Wk 3954	Witchcliffe Rock Shelter	400 (50)	400 (352-499)	Bone	27.86	293	8	√		
817	Wk 3954, Wk 3955	Witchcliffe Rock Shelter	400-680 (50-90)†	500 (352-706)	Bone	-	-				
818	Wk 3954, Wk 3955	Witchcliffe Rock Shelter	400-680 (50-90)†	500 (352-706)	Bone	23.86	293	3	√		
807	Wk 3954	Witchcliffe Rock Shelter	400 (50)	400 (352-499)	Bone	-	-				
820		Cranbrook		108	Skin	33.22	141				
821		Contine		44	Skin	28.25	293	7	√	√	√

Sample ID	C^{14} lab codes	Location	Uncalibrate Age (C^{14} error)	Age (year*)	Sample	Ct value	Largest Amplicon	Msat typed	BEAST BSP	Migrate-n BSP (mtDNA)	Migrate-n BSP (msats)
822		Pingelly		102	Skin	-	-				
823		Dwarladine Pool		102	Skin	29.2	293	8	√	√	√
824		Beaufort		108	Skin	25.14	253				
825		Dwarladine Pool		102	Skin	34.38	141				
826		Gracefield		108	Skin	26.41	253	7			√
827		Jerramungup		41	Skin	19.26	293		√	√	
828		Beverley		77	Skin	-	-				
829		Mammoth Cave		96	Skin	24.2	293	10	√		
830		Mammoth Cave		96	Skin	29.15	293	4	√		
832		Capel/Uralla		79	Skin	32.57	141				
833		Chorkerup		72	Skin	-	-				
834		Beverley		77	Skin	-	293				
835		Pingelly/ Woyerling		49	Skin	32.32	293		√	√	
836		Pingelly		78	Skin	-	-				
837		Contine		44	Skin	14.83	293	10	√	√	√
838		Mooterdine		44	Skin	17.69	293	10	√	√	√
840		Mooterdine		44	Skin	22.87	293	10	√		√
841		Karridale		78	Skin	-	-				
842		Karridale		80	Skin	-	-				
843		Karridale		80	Skin	32.29	253				
844		Unknown location		66	Skin	28.78	141				
845		Contine		44	Skin	18.59	293	9	√	√	√
846		Cuballing		47	Skin	16.84	293	10	√	√	√
848		Manjimup		32	Bone	17.33	293	8	√	√	√
849		Boyup Brook		41	Bone	29.4	253	8			√
850		Dryandra		37	Bone	25.26	293	7	√	√	√
851		Bernier Is., uncertain		96	Bone	31.57	253				
852		Faure Island		n/a	Bone	29.58	123				
853		Manjimup		32	Bone	27.25	293	10	√	√	√

Sample ID	C^{14} lab codes	Location	Uncalibrate Age (C^{14} error)	Age (year*)	Sample	Ct value	Largest Amplicon	Msat typed	BEAST BSP	Migrate-n BSP (mtDNA)	Migrate-n BSP (msats)
854		Perup River		30	Bone	28.88	293		√	√	
855		Manjimup		32	Bone	23	293	10	√	√	√
1003		Peron Peninsula		n/a	Bone	-	293				
1004		Faure Island		n/a	Bone	40.33	-				
1005		Faure Island		n/a	Bone	-	253				
1006		Faure Island		n/a	Bone	29.8	293				
1007		Nullarbor (cave)		n/a	Bone	-	-				
1008		Nail Tail Cave		n/a	Bone	35.37	-				
1009		Nullarbor (cave)		n/a	Bone	-	-				
1010		Nullarbor (cave)		n/a	Bone	42.95	253				
1011		Peak Charles N.P.		n/a	Bone	-	-				

* Years prior to 2008. Archaeological dates (i.e. more than 150 years) are based on calibrated radiocarbon age estimates of years before 1950. Between brackets range with ± s.e.

† Sample is positioned in an undated layer between two dated layers

Calibrations were carried out using CalPal2007_HULU calibration curve of the Cologne Radiocarbon Calibration & Paleoclimate Research Package, available at http://www.calpal-online.de/